International Journal of Chemical and Biochemical Sciences
(ISSN 2226-9614)

Journal Home page: www.iscientific.org/Journal.html

A simple preparation of hydroxyapatite/rice husk composite for efficient removal of heavy metal ions and textile dye

Thi Hong Anh Nguyen[1], Thi Hoai Nguyen Vo[2], Van Cuong Nguyen[2]*

[1]*Faculty of Chemical Engineering, Ho Chi Minh City University of Industry and Trade, Ho Chi Minh City, 70000 Viet Nam*

[2]*Faculty of Chemical Engineering, Industrial University of Ho Chi Minh City, Ho Chi Minh City, 70000 Viet Nam*

Abstract

This research presents a novel method for producing hydroxyapatite modified partly hydrolyzed rice husk (HAp/RH), which is then used to filter out heavy metals and dyes from water. The hydrochloric acid was used to break down half-chain of cellulose in the rice husk at 100ºC for 6h. The partial hydrolyzed rice husk surface was then covered with thin layer of hydroxyapatite. The as-synthesized HAp/RH was differentiated by FTIR, XRD and SEM, then studied for elimination of copper (II), nickel (II) ions and Sunfix Supra Red S3B 150% dyestuff. The result showed that the optimal condition for the hydrolysis of rice husk in 5% HCl an aqueous solution. The maximum removal efficiencies were ~ 99 and 70% for copper (II) and nickel (II) ions, respectively. Additionally, the removal efficiencies of copper (II) and nickel (II) ions from industrial wastewater by HAp/RH were 99.3% and 61.9% for 120 min, respectively. The result also indicated that 99.3% of the Sunfix Supra Red S3B 150% was removed after 150 min at initial concentration of 10 mg/L. According to the results of this research, HAp/RH shows promise as an adsorbent for the elimination of metal ions and textile colors.

Keywords: Rice husk, Hydroxyapatite, Heavy metal ions, Textile dyes, Adsorption.

Full length article **Corresponding Author*, e-mail: nvc@iuh.edu.vn

1. Introduction

Rice husk is produced as a byproduct of growing and milling rice (RH). It is significant to note that amorphous silica and carbon are both present in rice husk. These are porous materials with enormously high specific surface areas that can be applied to a wide range of situations [1]. The rice husk contains approximately 75% volatile organic matter that was burned during combustion and 25% inorganic matter [2]. The main organic components of rice husk are cellulose content (38-50%), hemicellulose (23-32%) and lignin (15-25%) [1]. From rice husk, lignin and hemicellulose could be isolated and hydrolyzed using a base and acid solution [3-4]. About 94 wt% of the inorganic stuff was silica, and 6 wt% comprised oxides of potassium, calcium, manganese, magnesium, aluminum, and phosphorus [5]. Rice husk was used as a promising source of biofuels, bioplastics production, adsorption of textile dye and heavy metal from wastewater [6]. Heavy metals are non-biodegradable, non-toxic when they are free elemental form and dangerous to living organisms in cationic form due to their ability to bind to short carbon chains leading accumulation in the organism after many years [7]. Due to the toxicity of heavy metal pollution, which endangers the aquatic life and puts human health at risk, it has become critical in many estuaries and coastal regions around the world [8-9]. Moreover, heavy metal and organic dyes pollution in wastewater have increased recently owing to the expanding global population and industrialization [10]. It is important to avoid the exposure to these pollutions to the environment. There are many methods for treating heavy metals and organic dyes, including adsorption, ion exchange, membrane filtration, flocculation, advanced oxidation and chemical precipitation [11-13]. Among all the adsorption method is frequently utilized because of its inexpensive, easily accessible materials, high adsorption capacity, and repeatability [9]. It is a well-known fact that the surface of rice husk is uneven therefore it might facilitate for the adsorption of metals and other contaminants. Additionally, RH has been utilized to treat wastewater in many places across the world since it has been found to effectively absorb metal ions and organic contaminants [14-15].

In this study, the rice husk was hydrolyzed to reduce the cellulose chain and create a silica film on the rice husk surface, then the layer of hydroxyapatite material was deposited on the rice husk's layer so as to increase the adsorption capacity of metal ions and solution-based dye.

2. Materials and methods

2.1. Materials

Rice husk was taken from a Giang province (Vietnam). $CuSO_4$, Ni $(NO_3)_2$, HCl (36wt%), NaOH, Ca $(OH)_2$, and H_3PO_4 (98wt%) were as analytical grade without further purification. Sunfix Supra Red S3B 150% textile dye was donated from 7-Textile Company (Vietnam). The anhydrous $CuSO_4$ and Ni $(NO_3)_2$ were dissolved in deionized water to make 1000 ppm copper (II) and nickel (II) solutions, respectively. After that, a standard solution was manufactured by diluting the stock solution until it reached the desired concentration. The wastewater at the plating factory was collected from Bien Hoa II Industrial Park, Dong Nai province, Vietnam.

2.2. Methods

2.2.1. Preparation of hydrolyzed rice husk (RH)

Rice husk was given a wash in double-distilled water to get rid of the dust, and then it was heated to one 100ºC to dry. Amount of 0.5 g RH was added to 250 mL of HCl (36wt (%) solution in round bottom flask. The combination was subjected to refluxing for a duration of 6 h. The hydrolyzed RH was neutralized using 1N NaOH solution to pH 7.0. Hydrolyzed RH was produced by filtering, washing, and drying the solid product with double-distilled water. The HCl concentration was 1, 2.5, 5, and 10% and sample was referred as RH.

2.2.2. Synthesis of hydroxyapatite modified RH (HAp/RH)

The preparation of HAp/RH was prepared by co-precipitation method. 10 g of hydrolyzed RH was inserted into100 mL deionized water containing 0.5g Ca $(OH)_2$, and then 0.3 mL H_3PO_4 was drop-wised to solution under continuously agitation. The pH level was brought up to 8.5 with the use of 0.1 N NaOH solution, and then it was filtered. The final product was dried under vacuum at 45ºC until constant weight.

2.2.3. Adsorption experiments

2.2.3.1. Adsorption of copper (II) and nickel (II)

Adsorptions of copper (II) and nickel (II) ions were investigated at room temperature in a batch setting, with adsorbent amounts ranging from 0.1 to 1.0 g. In brief, the HAp/RH adsorbent was added to 50 mL of single metal ion solution (20 mg/L). After that, the mixes were left at room temperature for 100 min under continuous stirring. The concentrations of copper (II) and nickel (II) ions in aqueous samples were measured by means of AAS. The effect of contact time was analyzed at metal ion concentrations of 20 mg/L, adsorbent doses of 0.5 g, and time intervals ranging from 0 to 480 min. Metal ion concentrations were determined by withdrawing aqueous samples at various time intervals. Furthermore, the effect of concentration was tested for 100 min at concentrations ranging from 5 to 30 mg/L. The adsorption yield was determined by $(C_0 - C_e)/C_0 \times 100$, Here, C_0 and C_e represent the initial and equilibrium concentrations of metal ions in the solution (mg/L). Metal ion removal from real industrial wastewater was determined using 0.5 g of HAp/RH adsorbent in 50 mL of industrial wastewater for 2 h at room temperature. The levels of copper (II) and nickel (II) ions in the remaining solutions were assessed using the AAS technique.

2.2.3.2. Adsorption of Sunfix Supra Red S3B 150% dye

Adsorbent dosages of 0.1, 0.2, 0.25, 0.5, and 0.75 g were evaluated to determine their influence. Each 100 mL of Erlenmeyer flask containing the determined amount of adsorbent was added 50 mL of Red S3B dye at an initial concentration of 50 mg/L. The resulting mixtures were being stirred at a rate of 150 rpm. UV-VIS spectroscopy at 540 nm determined dye concentration. The impact of the initial concentration and the duration of contact was examined in a 50 mL Red S3B dye solution with concentrations of 10, 20, 30, 40, 50, 75, and 100 mg/L, adsorbent amount of 0.5 g, and adsorption time ranging from 0 to 250 min.

2.3. Characterization

The specimens were analyzed using Fourier-transform infrared spectroscopy (FT-IR) on a Tensor 27-Bruker instrument from Germany, covering a scanning range of wave numbers between 400 and 4000 cm^{-1}. X-ray powder diffraction (XRD) was employed with a LabX XRD-6100 apparatus from Shimadzu in Japan to investigate the structural attributes of the produced materials. Additionally, the surface characteristics were assessed using scanning electron microscopy (SEM) with a HITACHI-S-4800 instrument from Tokyo, Japan.

3. Results and Discussion

3.1. Preparation and characterization

RH was hydrolyzed for 6 h at 100ºC with varying concentrations of HCl (1, 2.5, 5, and 10 wt%). The surface of the rice husk was rougher after hydrolysis process. Furthermore, the weight retention of rice husk decreased as the HCl concentration increased. For HCl concentrations of 1, 2.5, 5, and 10%, the mass loss of RH was 28, 33, 56, and 57%, respectively. The mass loss at 5 and 10 wt% HCl was comparable to the total hemicellulose and cellulose content in rice husk (54%) [16]. The results showed that all hemicellulose and amorphous cellulose are hydrolyzed [17]. As a result, rice husks hydrolyzed with 5 wt% HCl were chosen for future experiments. The surface of hydrolyzed rice husk (RH) was coated with hydroxyapatite using the co-precipitation method of Ca $(OH)_2$ and H_3PO_4 to form HAp/RH. The results of the FT-IR and XRD studies the structure of synthetic materials. Figure 1 demonstrates the broad absorption band at 3376 cm^{-1}, which is attributed to –OH stretching vibrations. The bending of C-H is represented by a weak peak at 2915 cm^{-1}. The absorption band at 1512 cm^{-1} is assigned to lignin, and its intensity increased after the RH was treated with HCl. The strong absorption bands at 1040 ~1104 cm^{-1} are attributed to the hemicelluloses and cellulose structures. Due to the hemicellulose in RH was hydrolyzed by HCl solutions, the strength of these peaks was reduced with increasing HCl concentration [18].

The intensity of the 805 cm^{-1} absorption band is due to symmetric stretching between Si-O-Si. Furthermore, Figure 1 shows the peaks at 1600~1641 cm^{-1} corresponding to C=C stretching of aromatic and benzene rings in lignin [19]. All of the absorption bands observed in the HCl-treated RH spectra were presented in the HAp/RH spectra indicating that they have similar compositions. Additionally, the asymmetric stretching vibrations of PO_4^{3-} were at 1039, 960, 609 and 567cm^{-1} belonging to HAp [20]. Figure 2 displays the XRD patterns obtained from the RH and HAp/RH samples. It is possible to suppose that the major characteristic peak for RH, which ranges from 20 to 25.2° and is centered at 22.8°, corresponds to the overlapped peaks of amorphous lignin and amorphous silica [17]. The main characteristic peak for RH ranged from 20 to 25.2 o and was centered at 22.8°, which could be attributed to overlapping amorphous lignin and amorphous silica peaks [4]. With increasing HCl concentration, the intensity of the peak at 22.8° decreases significantly. The XRD result showed peaks at 2θ values of 16.2 and 34.2°, which are attributed to the crystal structure of cellulose. In addition, the intensity of these peaks decreased as the HCl concentration increased. As a result of the more extensive elimination of cellulose and hemicelluloses through acid treatment, the treated sample displays elevated levels of lignin concentrations in contrast to the unprocessed sample. Furthermore, the XRD of HAp/RH shows all the peaks of RH as well as new HAp peaks at 26 and 32° [21]. Figure 3 displays SEM images of both the untreated and acid-treated RH. An ordinated cellulose structure with repeating regular and geometrical features defines the morphology of raw RH. The asperities were found in raw RH and were eliminated by HCl treatment. The acid-treated RH underwent a considerable alteration in surface structure. The surface of the acid-treated RH was relatively rough because the acid solutions had corroded it. The hydrolysis of cellulose and hemicellulose may be responsible for the difference in surface properties. The presence of silica particles was also observed in acid-treated RH [15]. Furthermore, silica particles appeared on the surface of RH hydrolyzed with 5 wt% HCl acid rather than 1 wt% HCl. Moreover, the surface of the HAp/RH appeared uneven and cracked. The HAp particle was deposited on the surface of the treated rice husk. As seen in Figure 3d, a thin layer of HAp made of tiny needle-like crystals that were organized in a coral-like structure was applied to the surface of acid-treated RH. The surface area and porosity of the HAp/RH were computed through the Brunauer-Emmet-Teller (BET) technique, employing the N_2 gas adsorption approach with a Nova Station A BET Surface Area Analyzer (Quantachrome Instruments). This analysis involved adsorption of N_2 at a temperature of 77.3 K. The outcomes indicate that the created samples exhibit isotherms classified as type IV in accordance with the IUPAC (International Union of Pure and Applied Chemistry) standards. This classification signifies a characteristic combination of micropores and mesopores. The specific surface area value and pore volume of composite are 37.1 m^2/g and 0.011 cm^3/g, repsectively.

3.2. Removal of metal ions

3.2.1. Influence of adsorbent amount

The adsorbents' mass is an essential factor in the process of adsorption. Figure 4 demonstrates the number of adsorbent increases; the adsorption of Cu (II) and Ni (II) ions increases progressively. Higher adsorption efficiency was observed at higher amounts of adsorbent due to greater availability of active sites on the surface area [8,22]. The removal percentage of Cu (II) ion increased from 71.67 to 93.3% as HAp/RH adsorbent increased from 0.01 to 0.5 g. The removal percentage reached equilibrium after 0.5 g of adsorbent, and the maximum removal efficiency was 98.56 at 1.0 g of adsorbent. Nevertheless, under equivalent adsorbent quantities, the adsorption effectiveness for Ni (II) ions was found to be inferior to that of Cu (II) ions. The removal efficiency was 64.10% for 0.5 g of HAp/RH adsorbent and reached a maximum of 70% for 1.0 g of HAp/RH adsorbent.

3.2.2. Influence of time and initial concentration

The significance of adsorption duration is widely recognized in the adsorption procedure. The impact of varying adsorption periods on the capacity for adsorption was explored over a span ranging from 0 to 480 min under room temperature conditions. In this investigation, the adsorbent quantity and the concentrations of metal ions were standardized at 0.5 g and 20 mg/L, respectively. Figure 5 shows that adsorption capacity increased rapidly from 0-380 min, then became almost constant, and reached equilibrium at time of 300 min for both Cu (II) and Ni (II) ions. Cu (II) adsorption efficiency increased from 26.6 to 70% for contact times ranging from 15 to 200 minutes, reaching a peak at 90% for 300 min. However, the adsorption efficiency of Ni (II) was 48.7% after 200 min and reached a maximum of 66.7% after 300 min. The higher adsorption of Cu^{2+} onto HAp/RH in comparion with Ni^{2+}. This can explain due to the exchange of Cu^{2+} with Ca^{2+} ions of HAp and its surface complexation with HAp in mixed metal suspension. The smilar result was obeserbed by Zou and cor-workers [22]. Remarkably, it is observed that elevating the initial concentration (ranging from 5 to 30 ppm) of Cu (II) and Ni (II) ions led to a reduction in the adsorption effectiveness of HAp/RH, as depicted in Figure 6. This is because of the effects of mass transfer and the driving power of the concentration gradient, which is directly related to the concentrations at the initial stage [23-24]. The percentage removal for 5 mg/L of Cu (II) and Ni (II) ions was 88 and 75%, respectively. However, at 30 mg/L of Cu (II) and Ni (II) ions the percentage removal decreased to 61 and 42%, respectively. The adsorption mechanism is physical adsorption followed by chemical adsorption. The first step was to perform a rapid surface adsorption on the HAp/RH composite. The second step was ion exchange with ion metal, followed by precipitation of the ion metal. Based on results show that the adsorption capacity of the HAp, and rice husk, the ion metal adsorption and color removal of HAp/RH is higher than those of HAp, and rice husk. For Cu^{2+} ion, adsorption efficiency was 68 and 35% for the HAp, and rice husk, respectively while the removal for composite was 93.3%. The industrial wastewater was collected from plating factory in Bien Hoa II Industrial Park, Vietnam. AAS was used to determine the Cu (II) and Ni (II) concentrations in effluent. Cu (II) and Ni (II) concentrations in the effluent were diluted to 25.53 and 27.7mg/L, respectively. Adsorption efficiency of HAp/RH towards Cu (II) was 99.3% while the one towards Ni (II) was 61.9%.

The results of this study imply that HAp/RH could be used to treat wastewater by removing heavy metal ions.

3.2.3. Adsorption of Sunfix Supra Red S3B 150%

The effect of HAp/RH dose on Sunfix Supra Red S3B 150% dye removal efficiency was studied by employing adsorbents at concentrations ranging from 0.1 to 1.0 g while maintaining the volume (50 mL) and dye concentration (20 mg/L). As shown in Figure 7, Sunfix Supra Red S3B 150% dye adsorption onto HAp/RH increased from 50.1 to 87.9% for adsorbent doses of 0.1 to 0.5 g, respectively. At higher amount of 0.5 g, the removal percentage reached equilibrium. Due to the larger concentration of adsorbents in the solution and the greater availability of active sites for the dye molecules, the maximum removal was 98% for an adsorbent quantity of 0.75 g [25]. Figure 8 depicts the adsorption yield as a function of initial concentration and contact time. The adsorption efficiency increased rapidly in the first 50 min, then became nearly constant and reached equilibrium after 100 min. Furthermore, the adsorption efficiency decreased as the initial dye concentration increased from 50 to 100 mg/L, possibly due to a decrease in the number of available active sites of the adsorbent. Adsorption yields ranged from 99.3 to 17.7% for dye solutions with initial concentrations ranging from 10 to 100 mg/L. These findings confirm that the initial dye concentrations played a significant role in composite adsorption. The high removal yield at low concentration could be attributed to dyes moving more quickly into the active sites of the composite. The removal of reactive dyes from wastewater yielded similar results [26]. From this experiment showed that the combination of HAp and rice husk increases dye adsorption capacity to 98% in comparion to unmodified materials (76% for rice husk and 82% for HAp).

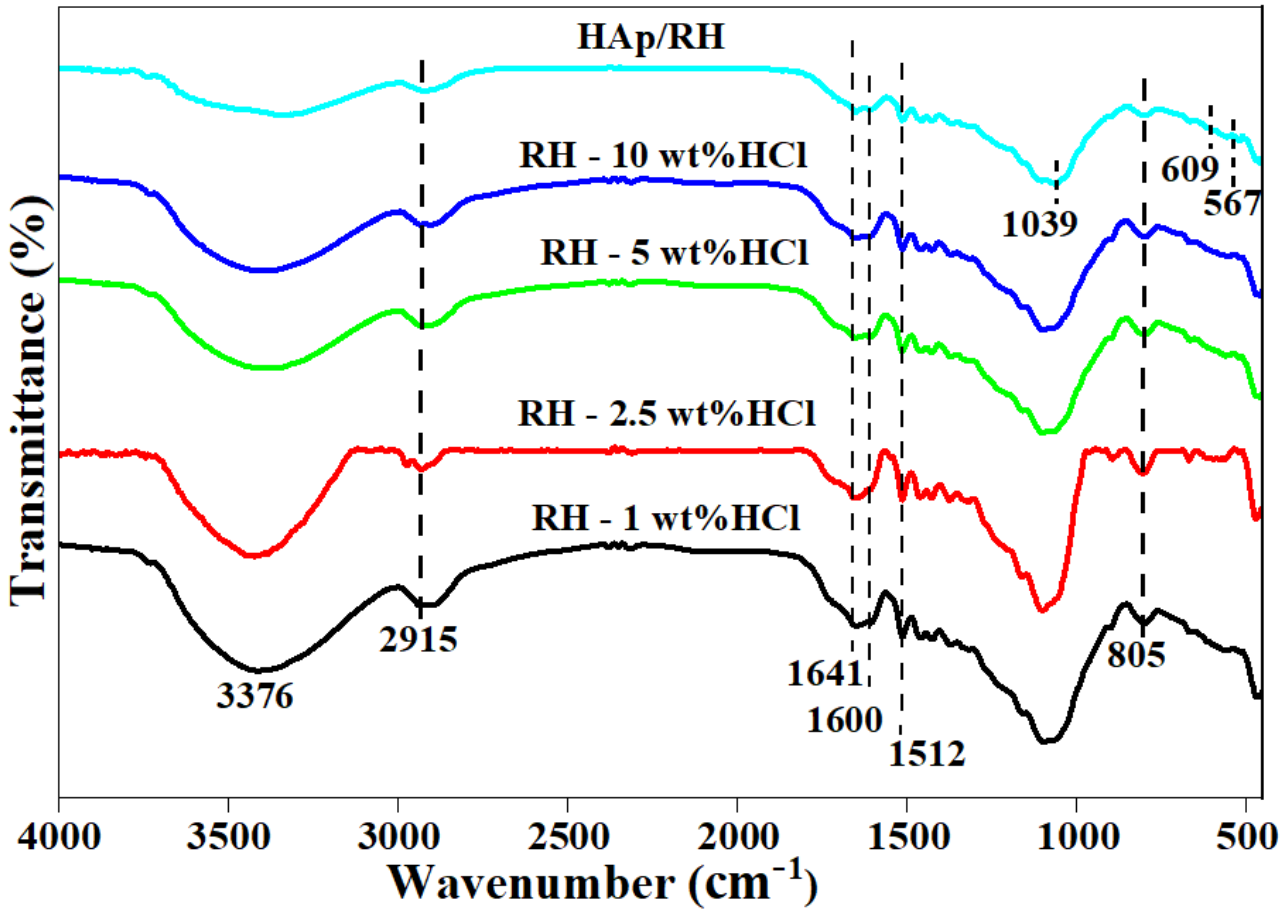

Figure 1: FT-IR of hydrolyzed RH at various HCl concentration and HAp/RH.

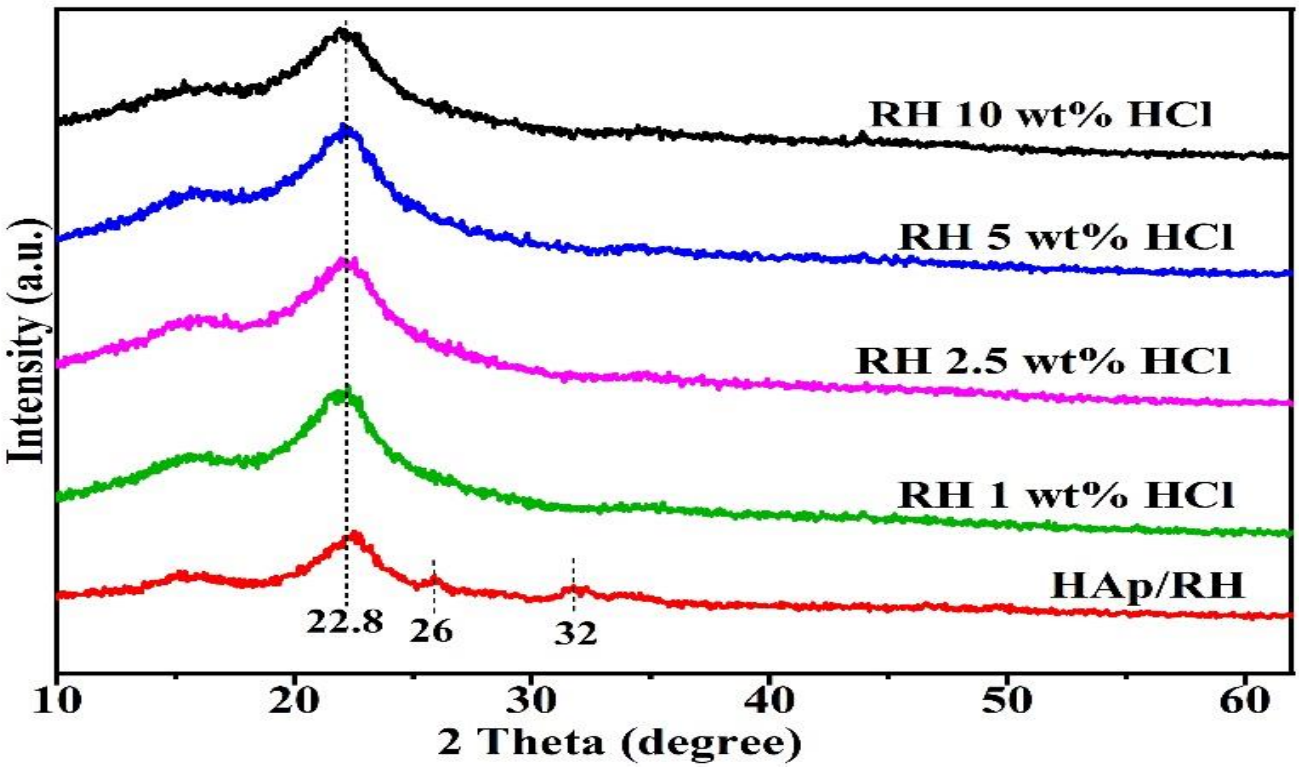

Figure 2: XRD of hydrolyzed RH at various HCl concentration and HAp/RH.

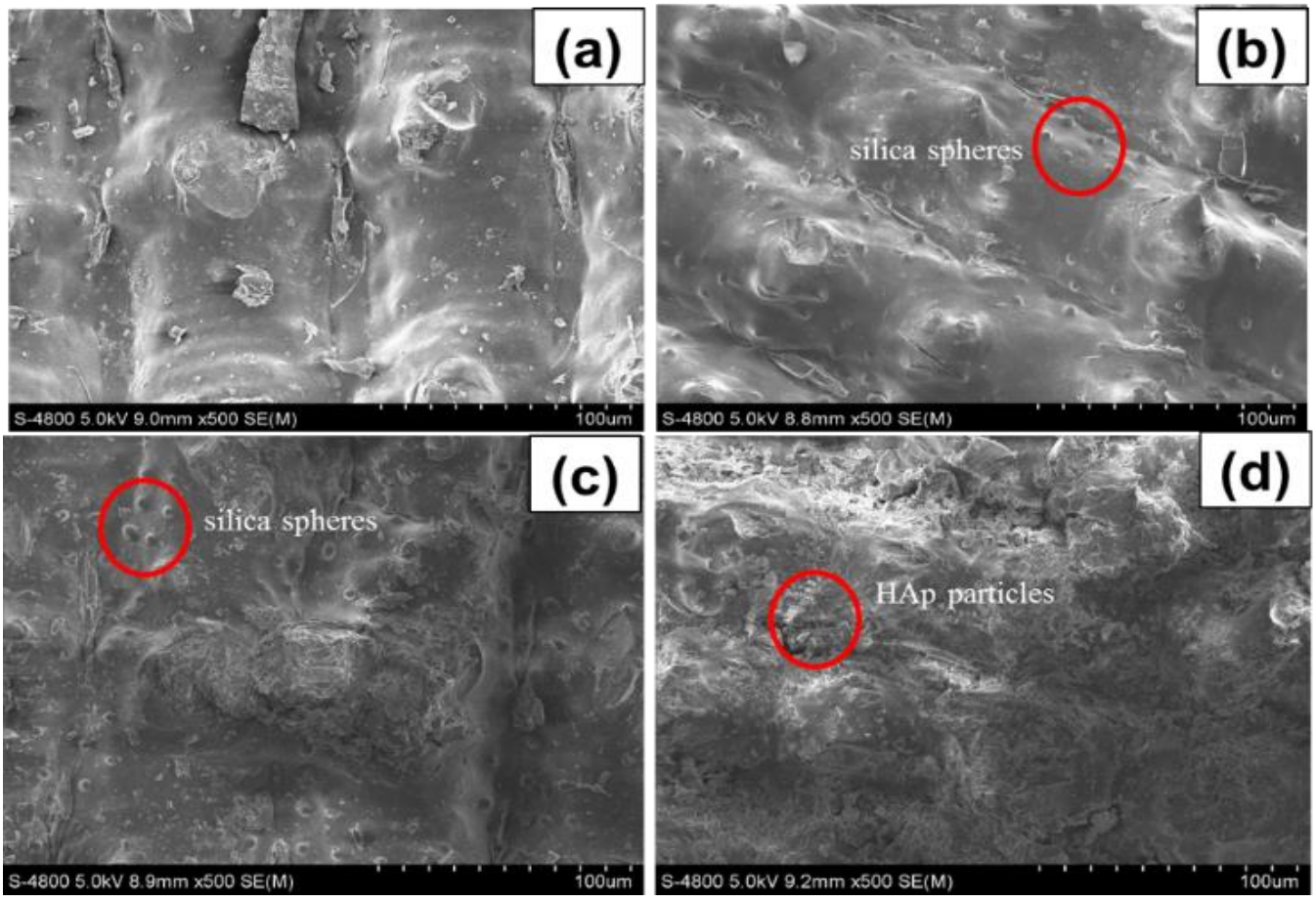

Figure 3: SEM images of untreated RH (a), hydrolyzed RH using HCl 1 wt% (b), 5 wt% (c), and HAp/RH using HCl 5 wt% (d).

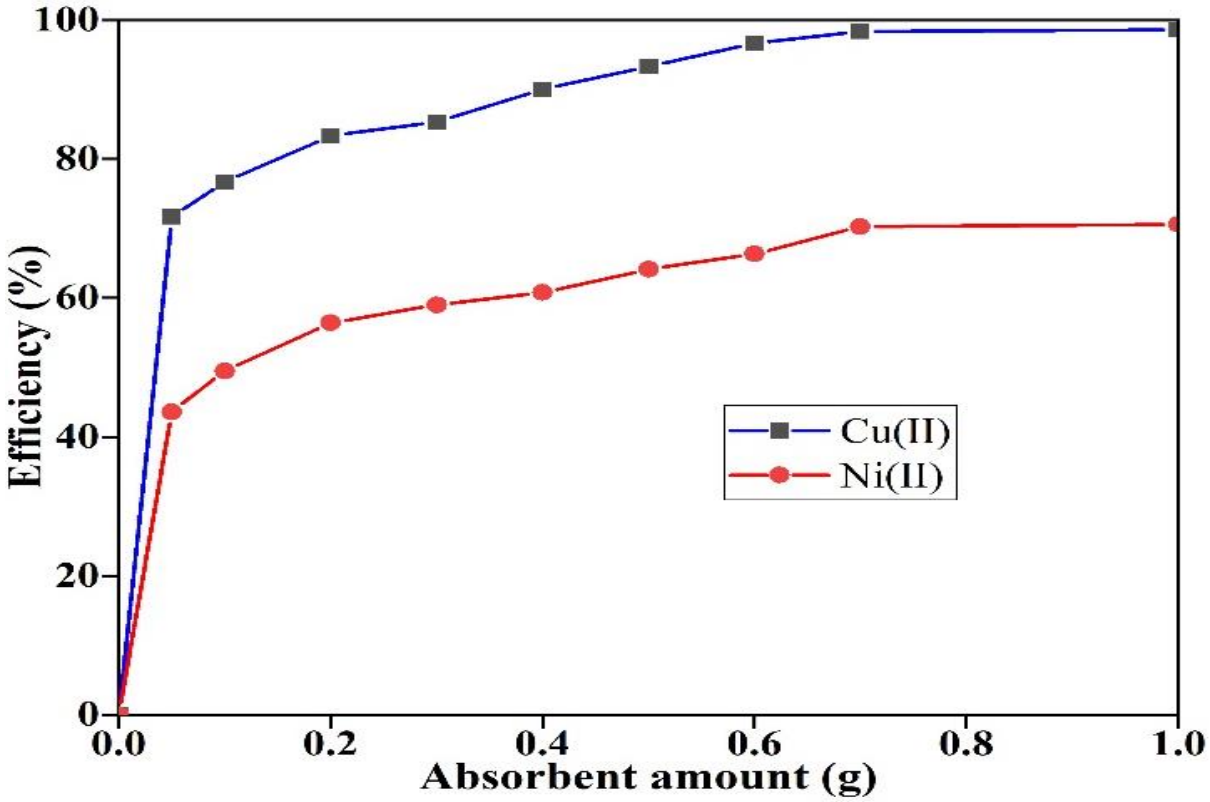

Figure 4: Effect of adsorbent amount to adsorption capacity of HAp/RH towards Cu(II) and Ni(II) ions (50 mL metal ion solution of 20 mg/L and time of 100 min).

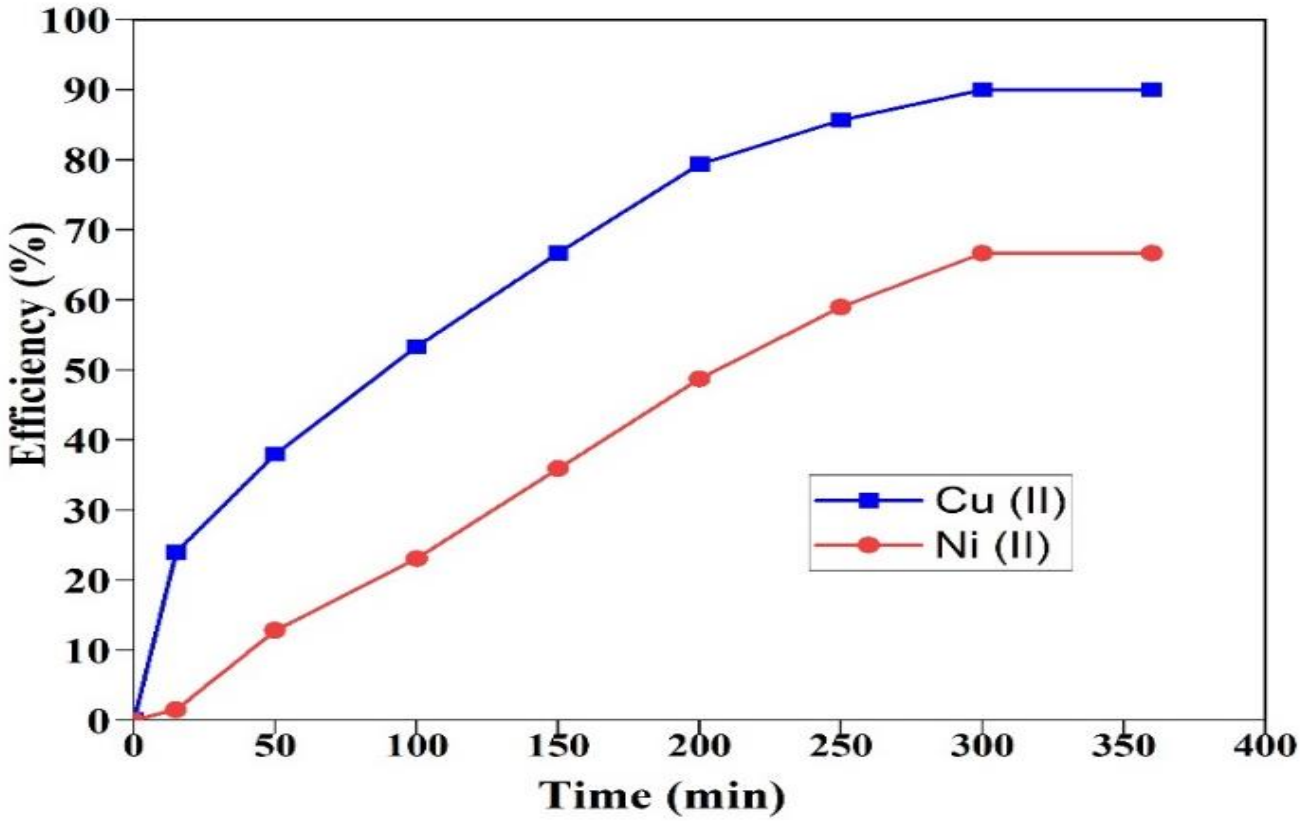

Figure 5: Effect of contact time to adsorption efficiency of HAp/RH towards Cu(II) and Ni(II) ions (50 mL metal ion solution of 20 mg/L and 0.5 g of HAp/RH).

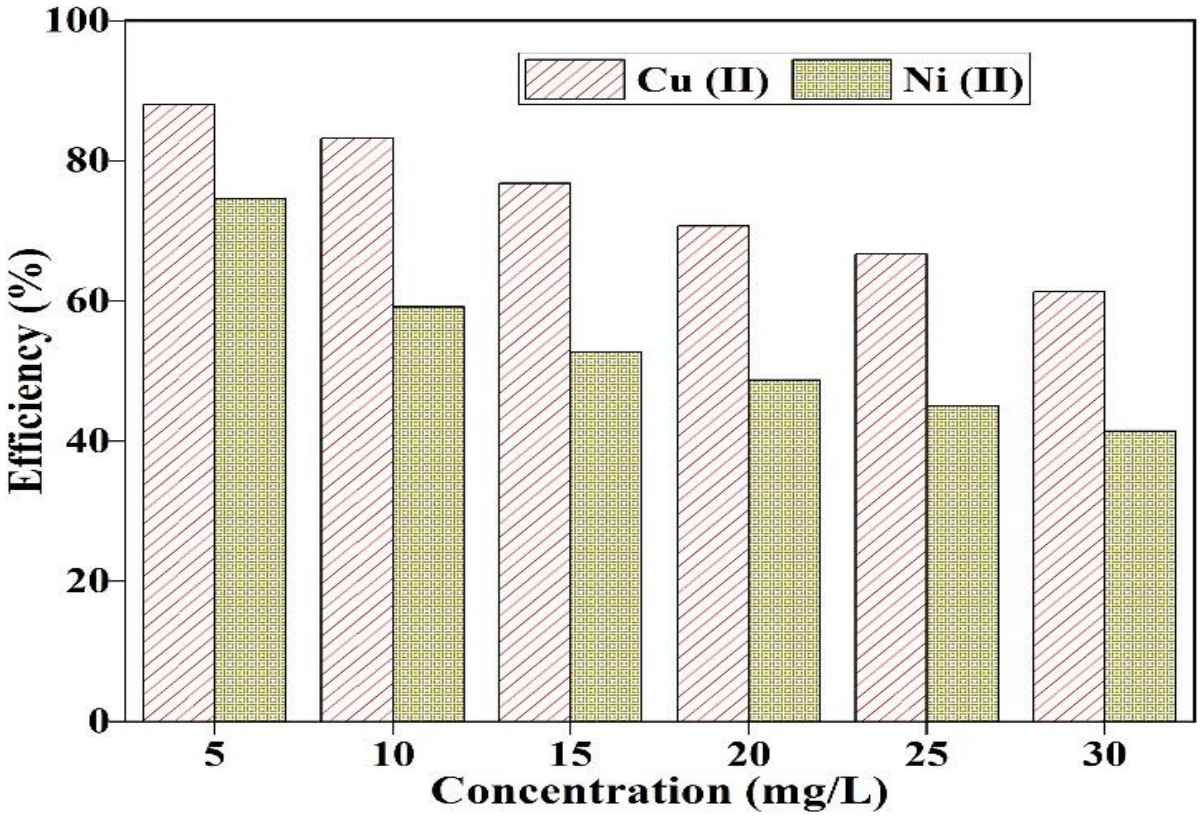

Figure 6: Effect of initial concentration of metal ions to adsorption efficiency of HAp/RH towards Cu (II) and Ni (II) ions (0.5 g of HAp/RH, and 100 min of contact time).

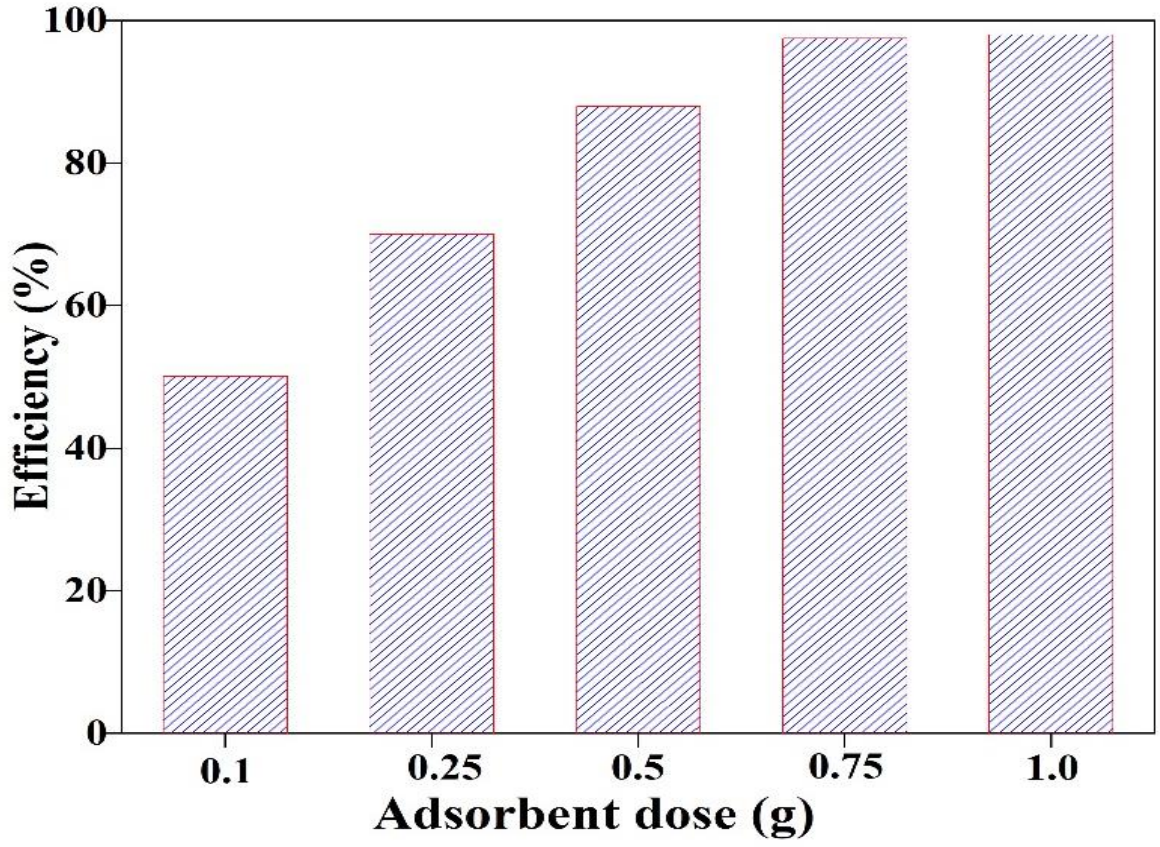

Figure 7: Effect of adsorbent dose to adsorption efficiency of HAp/RH towards Sunfix Supra Red S3B 150% dyestuff.

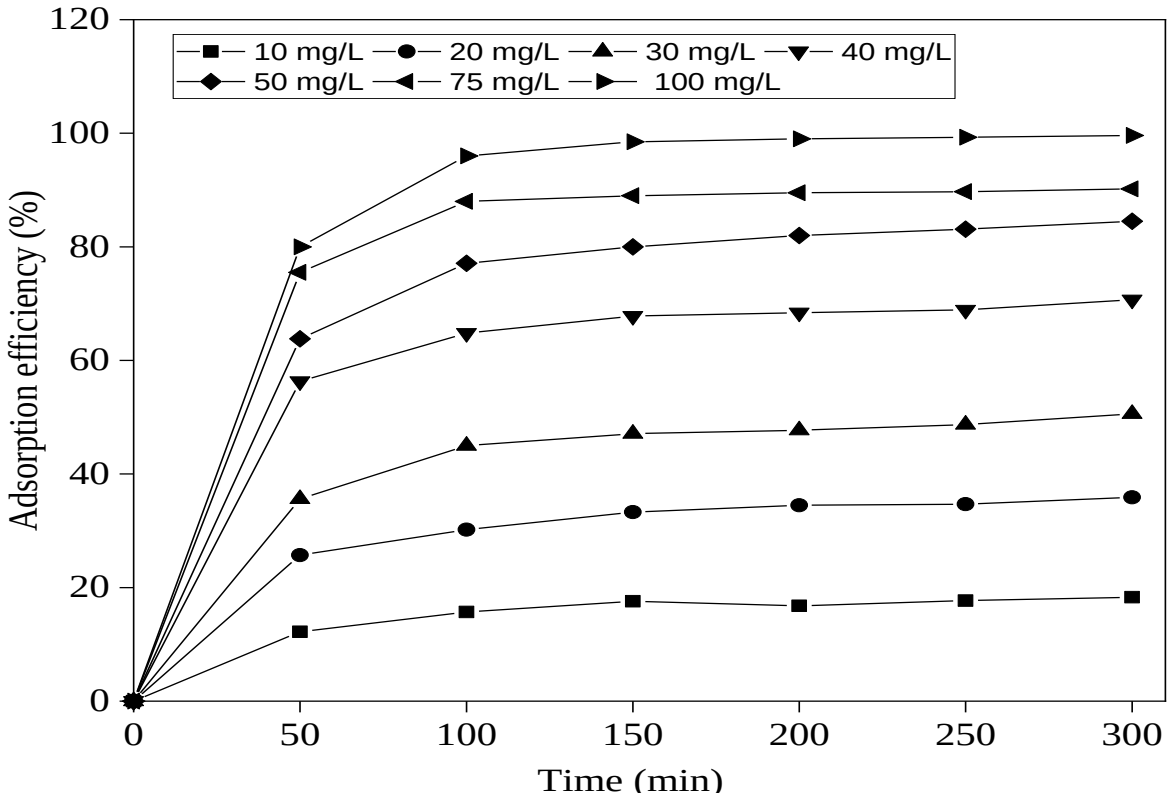

Figure 8: Effect of initial concentration and contact time to adsorption efficiency of HAp/RH towards Sunfix Supra Red S3B 150% dyestuff.

4. Conclusions

In the current study, rice husk was hydrolyzed using various HCl acid concentrations, and subsequently coated with HAp. The as-synthesized HAp/RH was utilized for removal of Cu (II), Ni (II), and Sunfix Supra Red S3B 150% dyestuff. The XRD and FT-IR results revealed that granular silica has an amorphous structure, and the presence of HAp was demonstrated on the surface of hydrolyzed RH. The adsorption process involving Cu (II), Ni (II), and Sunfix Supra Red S3B 150% dyestuff onto HAp/RH was analyzed, revealing a reliance on dosage, initial concentration, and contact duration. Notably, the extraction of Cu (II) and Ni (II) ions from industrial wastewater using HAp/RH yielded removal rates of 99.3 and 61.9%, respectively. Additionally, the results indicated that 99.3% of the Sunfix Supra Red S3B 150% was removed at initial concentration of 10 mg/L.

Acknowledgements

The author would like to thank the Ho Chi Minh City University of Industry and Trade and Industrial University of Ho Chi Minh City, Viet Nam for financial and facilities assistance.

References

[1] B. A. Goodman. (2020). Utilization of waste straw and husks from rice production: A review. Journal of Bioresources and Bioproducts. 5: 143–162. https://doi.org/https://doi.org/10.1016/j.jobab.2020.07.001.

[2] S. K. S. Hossain, L. Mathur, P. K. Roy. (2018). Rice husk/rice husk ash as an alternative source of silica in ceramics: A review. Journal of Asian Ceramic Societies. 6: 299–313. https://doi.org/10.1080/21870764.2018.1539210.

[3] H. Asadi, M. Ghorbani, M. Rezaei-Rashti, S. Abrishamkesh, E. Amirahmadi, C. Chengrong, M. Gorji. (2021). Application of Rice Husk Biochar for Achieving Sustainable Agriculture and Environment. Rice science. 28: 325–343. https://doi.org/10.1016/J.RSCI.2021.05.004.

[4] Q. L. Hao, B. L. Li, L. Liu, Z. B. Zhang, B. J. Dou, C. Wang. (2015). Effect of potassium on pyrolysis of rice husk and its components. Journal of Fuel Chemistry and Technology. 43: 34–41. https://doi.org/10.1016/S1872-5813(15)60006-8.

[5] N. H. M. Muzni, N. H. Jamil, F. C. Pa, W. M. Arif. (2020). Effect of Acid Leaching on Different State of Rice Husk. Materials Science Forum. 1010: 532–537. https://doi.org/10.4028/www.scientific.net/MSF.1010.532.

[6] H. K. Okoro, S. M. Alao, S. Pandey, I. Jimoh, K. A. Basheeru, Z. Caliphs, J. C. Ngila. (2022). Recent potential application of rice husk as an eco-friendly adsorbent for removal of heavy metals. Applied water science. 12: 259. https://doi.org/10.1007/s13201-022-01778-1.

[7] M. Kapahi, S. Sachdeva. (2019). Bioremediation Options for Heavy Metal Pollution. Journal of Health and Pollution. 9: 191203. https://doi.org/10.5696/2156-9614-9.24.191203.

[8] R. Lakshmana Naik, M. Rupas Kumar, T. Bala Narsaiah. (2022). Removal of heavy metals (Cu & Ni) from wastewater using rice husk and orange peel as adsorbents. Materials Today: Proceedings. https://doi.org/https://doi.org/10.1016/j.matpr.2022.06.112.

[9] P. S. Kumar, R. Gayathri, B. S. Rathi. (2021). A review on adsorptive separation of toxic metals from aquatic system using biochar produced from agro-waste. Chemosphere. 285: 131438. https://doi.org/10.1016/J.CHEMOSPHERE.2021.131438.

[10] H. Xiang, X. Min, C. J. Tang, M. Sillanpää, F. Zhao. (2022). Recent advances in membrane filtration for heavy metal removal from wastewater: A mini review. Journal of Water Process Engineering. 49: 103023. https://doi.org/https://doi.org/10.1016/j.jwpe.2022.103023.

[11] Y. Dong, X. Kong, X. Luo, H. Wang. (2022). Adsorptive removal of heavy metal anions from water by layered double hydroxide: A review. Chemosphere. 303: 134685. https://doi.org/https://doi.org/10.1016/j.chemosphere.2022.134685.

[12] M. Shabir, M. Yasin, M. Hussain, I. Shafiq, P. Akhter, A. S. Nizami, B. H. Jeon, and Y. K. Park. (2022). A review on recent advances in the treatment of dye-polluted wastewater. Journal of Industrial and Engineering Chemistry. 112: 1–19. https://doi.org/https://doi.org/10.1016/j.jiec.2022.05.013.

[13] T. N. M. An, T. T. Phuc, D. N. T. Nhi, N. Van Cuong. (2020). Removal of reactive red dye by reusable chitosan-polyaniline/Fe3O4 nanocomposite. Vietnam Journal of Chemistry. 58: 477–481. https://doi.org/https://doi.org/10.1002/vjch.201900145.

[14] S. Yi, B. Gao, Y. Sun, J. Wu, X. Shi, B. Wu, X. Hu. (2016). Removal of levofloxacin from aqueous solution using rice-husk and wood-chip biochars. Chemosphere. 150: 694–701. https://doi.org/10.1016/j.chemosphere.2015.12.112.

[15] Z. Emdadi, N. Asim, A. Yarmo, K. Sopian. (2015). Effect of Chemical Treatments on Rice Husk (RH) Water Absorption Property. International Journal of Chemical Engineering. 6: 273–276. https://doi.org/10.7763/IJCEA.2015.V6.495.

[16] Y. López, A. Garcia, K. Karimi, M. J. Taherzadeh, C. Martin. (2010). Chemical characterization and dilute-acid hydrolysis of rice hulls from an artisan mill. Bioresource Technology. 5 (4): 2268-2277.

[17] L. Ma, L. Liu, X. Liu, Y. Li, Y. Feng, Y. Tian, Y. Chao, Y. Zhu, X. Wang. (2021). Acid Hydrolysis to Provide the Potential for Rice-Husk-Derived C/SiO2 Composites for Lithium-Ion Batteries. Journal of electronic materials. 50: 4426–4432. https://doi.org/10.1007/s11664-021-08965-x.

[18] M. Aminu. (2017). Acid Hydrolysis-Mediated preparation of Nanocrystalline Cellulose from Rice Straw. International Journal of Nanomaterials, Nanotechnology and Nanomedicine. 051–056. https://doi.org/10.17352/2455-3492.000021.

[19] T. N. Ang, G. C. Ngoh, A. S. M. Chua, M. G. Lee. (2012). Elucidation of the effect of ionic liquid pretreatment on rice husk via structural analyses. Biotechnology for biofuels and bioproducts. 5: 67. https://doi.org/10.1186/1754-6834-5-67.

[20] N. T. H. Anh, T. P. Trinh, L. V. Tan, N. T. M. Tho, N. V. Cuong. (2022). Facile synthesis of hydroxyapatite from bovine bone and gelatin/chitosan-hydroxyapatite scaffold for potential tissue engineering application. Vietnam Journal of Chemistry. 60: 198–205. https://doi.org/https://doi.org/10.1002/vjch.202100126.

[21] K. C. V. Kumar, T. J. Subha, K. G. Ahila, B. Ravindran, S. W. Chang, A. H. Mahmoud, O. B. Mohammed, M. A. Rathi. (2021). Spectral characterization of hydroxyapatite extracted from Black Sumatra and Fighting cock bone samples: A comparative analysis. Saudi journal of biological sciences. 28: 840–846. https://doi.org/https://doi.org/10.1016/j.sjbs.2020.11.020.

[22] X. Zou, Y. Zhao, Z. Zhang. (2019). Preparation of hydroxyapatite nanostructures with different morphologies and adsorption behavior on seven heavy metals ions. Journal of Contaminant Hydrology. 226: 103538. https://doi.org/https://doi.org/10.1016/j.jconhyd.2019.103538.

[23] S. Saber-Samandari, S. Saber-Samandari, N. Nezafati, K. Yahya. (2014). Efficient removal of lead (II) ions and methylene blue from aqueous solution using chitosan/Fe-hydroxyapatite nanocomposite beads. Journal of Environmental Management. 146: 481–490. https://doi.org/10.1016/J.JENVMAN.2014.08.010.

[24] F. Hassanzadeh-Afruzi, F. Esmailzadeh, S. Asgharnasl, F. Ganjali, R. Taheri-Ledari, A. Maleki. (2022). Efficient removal of Pb (II)/Cu (II) from aqueous samples by a guanidine-functionalized SBA-15/Fe3O4. Separation and Purification Technology. 291: 120956. https://doi.org/https://doi.org/10.1016/j.seppur.2022.120956.

[25] N. U. M. Nizam, M. M. Hanafiah, E. Mahmoudi, A. A. Halim, A. W. Mohammad. (2021). The removal of anionic and cationic dyes from an aqueous solution using biomass-based activated carbon. Scientific reports. 11: 8623. https://doi.org/10.1038/s41598-021-88084-z.

[26] V. Janaki, K. Vijayaraghavan, B. T. Oh, K. J. Lee, K. Muthuchelian, A. K. Ramasamy, S. Kamala-Kannan. (2012). Starch/polyaniline nanocomposite for enhanced removal of reactive dyes from synthetic effluent. Carbohydrate polymers. 90: 1437–1444.